Geofísica Internacional (2003), Vol. 42, Num. 1, pp. 25-39

Sedimentation conditions and rock-magnetic properties of Quaternary deposits from Laguna de Santa Rosa, Iturbide region, northeastern Mexico

J. Urrutia-Fucugauchi[1], M.A. Ruiz-Martínez[2], J. Werner[3], H.-W. Hubberten[4], T. Adatte[5], E. Escobar-Hernández[1], A. Arciniega-Ceballos[1], M. Hernández[2] and A. De León[3]

[1] *Laboratorio de Paleomagnetismo y Geofísica Nuclear, Instituto de Geofísica, UNAM, México, D.F., MÉXICO*
[2] *Facultad de Ciencias Forestales, Universidad Autónoma de Nuevo León, Nuevo León, MÉXICO*
[3] *Facultad de Ciencias de la Tierra, Universidad Autónoma de Nuevo León, Nuevo León, MÉXICO*
[4] *Alfred-Wegner Institut für Polar-und Meeresforschung, Forschungsstelle Potsdam, Potsdam, GERMANY*
[5] *Institut de Geologie, Université de Neuchâtel, Neuchâtel, SWITZERLAND*

Received: February 19, 2002; accepted: October 25, 2002

RESUMEN

Se reportan resultados iniciales del estudio interdisciplinario de la secuencia lacustre de Laguna Santa Rosa, en el núcleo de 26 m de longitud recuperado en el sector norte-centro. Santa Rosa es una cuenca intermontaña, con una reducida zona de captación, altitud de 1520 m snm, y situada en el sector central de la Sierra Madre Oriental en la región de Iturbide en el noreste de México. Las variaciones estratigráficas de las propiedades magnéticas, contenido total de carbonato y carbón isotópico y mineralógico, definen tres zonas separadas por incrementos del cociente de calcita a quarzo+phyllosilicatos+feldespatos. La zona más somera, desde la superficie hasta 7-9 m, está formada por arcilla orgánica con abundancia de gasterópodos y dos arcillas de color negro a verde. Se caracteriza por susceptibilidad magnética alrededor de 10^{-6} SI, factor de frecuencia de 0 %, δ^{13} C que abarca desde –20.3 ‰ a –26.4 ‰, presencia de cuarzo y phylosilicatos casi siempre con más de 20 % de calcita y esporádica aparición de plagioclasa (albita) y escaso contenido de K-feldespatos. La zona media, desde 9 m hasta 17.5 m, está formada por cinco unidades de arcilla que varían desde el verde grisáceo al café. Esta zona se caracteriza por su susceptibilidad variable arriba de 17 10^{-6} SI, factores de frecuencia negativos, bajo contenido total de carbonato, enriquecimiento de cuarzo y phylosilicatos, menos calcita y presencia de k-feldespatos. Esta zona media muestra un incremento en el aporte de detritos y/o productividad reducida, lo que sugiere un intervalo frío y menos húmedo. La zona más baja se extiende desde 17.5 m hasta 26 m y muestra dos unidades de arcilla que van del café al verde grisáceo. Esta zona se caracteriza por susceptibilidad magnética entre 8 10^{-6} SI y 14 10^{-6} SI, factor variable de frecuencia, y valores δ^{13} C de alrededor –24 ‰. Su mineralogía es similar a la de la zona más somera, también rica en calcita y aparición de plagioclasa. La porción de phylosilicatos está compuesta principalmente de micas, clorita, esmectita y kaolinita. Los minerales magnéticos son alogénicos, derivados de lutitas y carbonatos que forman la cuenca de la zona de captación.

PALABRAS CLAVE: Magnetismo de rocas, arcillas, Cuaternario, Laguna de Santa Rosa, noreste de México.

ABSTRACT

We report initial results of an interdisciplinary study of the lacustrine sequence of Laguna de Santa Rosa, based on a 26 m long core recovered from its northern-central sector. The Laguna is an intramontane elongated basin with a small catchment area at an altitude of 1520 m asl in the central sector of the Sierra Madre Oriental in the Iturbide region, northeastern Mexico. The stratigraphic variations of rock-magnetic properties, total carbonate content and isotopic carbon, and mineralogy define three major zones separated by peaks of the calcite to quartz+phyllosilicate+feldspar ratio. The upper zone, from surface to 7-9 m, is formed by an organic clay with abundant gasteropods and two black to green clays. It is characterized by magnetic susceptibility around 10^{-6} SI, frequency dependent factor of 0 %, δ^{13} C ranging from –20.3 ‰ at surface to –26.4 ‰, presence of quartz and phyllosilicates with generally more than 20 % calcite, and sporadic occurrence of plagioclase (albite) with K-feldspars nearly absent. The middle zone, from 9 m to 17.5 m, is formed by five clay units with colors ranging from green gray to brown. This zone is characterized by variable susceptibility up to 17 10^{-6} SI, negative frequency dependent factors, low total carbon content, quartz and phyllosilicate enrichment, less calcite and presence of K-feldspars. This middle zone shows higher detrital input and/or reduced productivity, which suggests a cold and less humid interval. The lower zone extends from 17.5 m to 26 m and shows two brown to green gray clay units. This zone is characterized by magnetic susceptibility between 8 10^{-6} SI and 14 10^{-6} SI, variable frequency dependent factors, and δ^{13} C values around –24 ‰. Its mineralogy is similar to the upper zone, again enriched in calcite and occurrence of plagioclase. The phyllosilicate fraction is mainly composed of mica, chlorite, smectite and kaolinite. The magnetic minerals are allogenic, derived from the lutites that form the catchment basin.

KEY WORDS: Rock-magnetism, clays, Quaternary, Laguna de Santa Rosa, northeastern Mexico.

INTRODUCTION

The arid and semi-arid region of northeastern Mexico (Chihuahuan Desert, the Sierra Madre Oriental and the Gulf Coastal Plain; Figure 1) is the focus of studies that attempt to unravel the paleoclimatic and paleoenvironmental evolution during the Quaternary. The region is highly complex due to the variation in elevation, mean temperature, precipitation, seasonal temperature fluctuations, and a variety of local factors. Nowadays, the region gets most of the precipitation during the summer, under the dominant influence of moist trade winds from the Atlantic ocean and Gulf of Mexico. These regional climatic conditions have probably prevailed during most of the Holocene. In the Late Pleistocene, during the last glaciation, conditions were probably different with Pacific ocean precipitation sources being dominant, producing increased winter precipitation (e.g., Bradbury, 1997). Paleoclimatic records are still scarce, particularly for the Sierra Madre Oriental and eastern Gulf Coastal Plain regions. The high topographic relief of the Sierra Madre Oriental (Figure 1) has played an important role in controlling precipitation and this topographic barrier produces complex local conditions.

In the Sierra Madre Oriental, lacustrine sediments can be found within intramontane basins and deeply incised valleys where small lakes were formed by karst subsidence (particularly in gypsum layers) or by catastrophic landslides that blocked the hydrological system. These paleolakes are of interest not only as paleogeographic elements of the Sierra Madre Oriental, but also for the potentially detailed records of Quaternary paleoclimatic and paleoenvironmental evolution (Ruiz-Martínez and Werner, 1997).

In this paper we present the initial results of a study of the lacustrine sequence of the Laguna de Santa Rosa. The Laguna de Santa Rosa is located in the central sector of the Santa Rosa canyon within the Sierra Madre Oriental (Figure 2). This study forms part of a long-term interdisciplinary project directed to investigate the Quaternary and paleoenvironmental and paleoclimatic evolution of northeastern Mexico. We report results for a 26 m long core drilled in the northern-central sector of the Laguna de Santa Rosa.

LAGUNA DE SANTA ROSA

Laguna de Santa Rosa is located within an elongated mountain basin in the region of Iturbide, the Sierra Madre Oriental. Laguna de Santa Rosa is oriented roughly northwest-southeast and drains into the larger east-west Santa Rosa canyon (Figure 2). Jurassic and Cretaceous sedimentary rocks form the elongated canyon that houses the Laguna. The local basement is probably formed by lutites of the middle

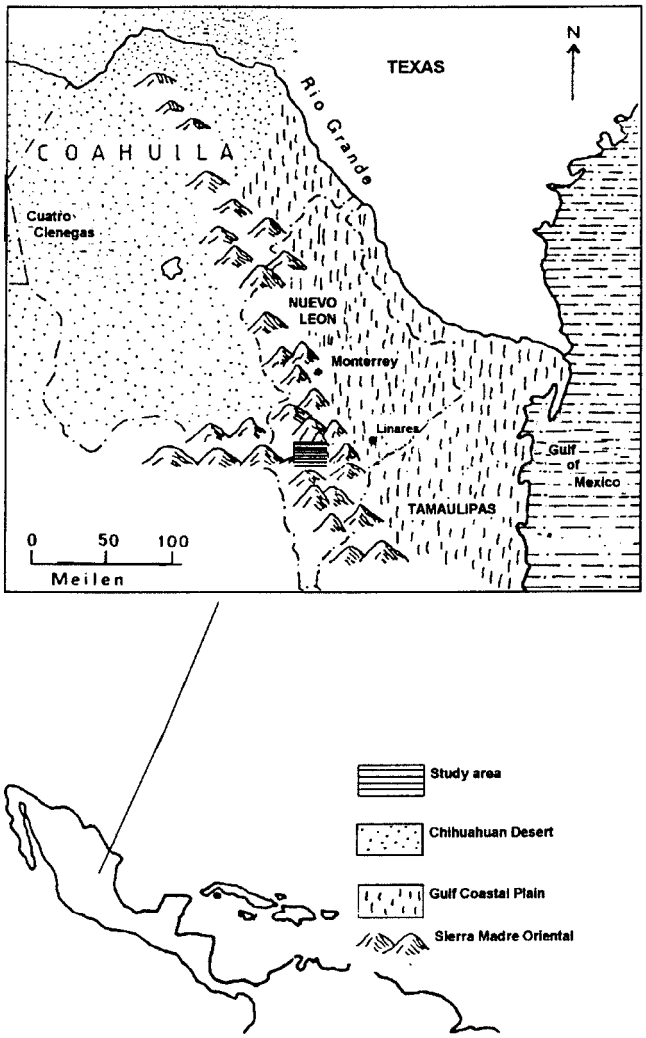

Fig. 1. Schematic map of northeastern Mexico with the Sierra Madre Oriental, the Gulf of Mexico coastal plain and the Chihuahuan Desert. The study area lies within the central sector of the Sierra in the Iturbide-Linares region.

Jurassic La Casita Formation, limestones of the Zuloaga Formation and evaporites of the Minas Viejas Formation (Figure 3). The lacustrine sequence accumulated in a karst depression formed at the core of the anticline structure. The lithologies that constitute the topographic highs in the catchement area are mainly limestones from the Taraises and Aurora Formations.

The study area lies within the fold and thrust belt of the Sierra Madre Oriental, formed during the Late Cretaceous-Early Tertiary (Laramide orogeny), which presents a regional trend NW-SE (Padilla y Sánchez, 1978). The mountain belt is conformed mainly by Mesozoic sedimentary units resting over a Paleozoic and Precambrian basement (Sánchez-Álvarez and Urrutia-Fucugauchi, 1992). The mean altitude of the region is around 2200 m asl (above sea level). The belt is characterized by an alternance of ranges and basins, with

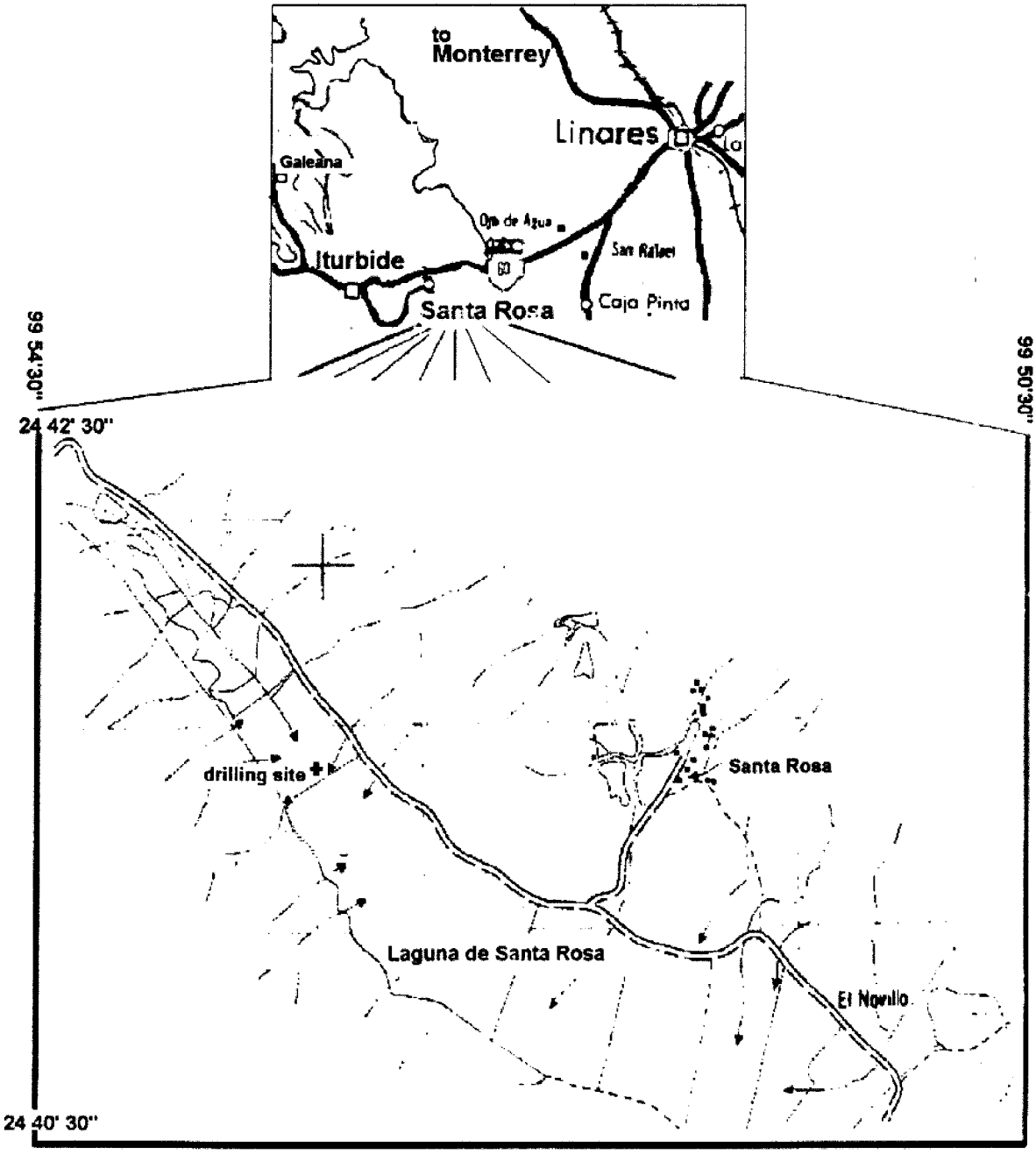

Fig. 2. Schematic map of the Laguna de Santa Rosa showing location of the drilling site.

steep slopes around 50° and up to 70°. Vertical scarps of folded limestone beds form the top and also the slopes of the ranges. The intermontane valleys are formed by dissection along zones of weakness at lithological contacts, fractures and axes of anticline/syncline structures.

The Santa Rosa river cuts the NNW-SSE structures of the Sierra Madre Oriental in an east-west direction (Carlsen, 1987). The river has cut the shales, lutites and limolites of the Maestrichtian Mendez Formation. East of the front of the Sierra, the Santa Rosa River drains along the Gulf of Mexico coastal plain. The mean altitude of the plain at the mountain front is around 1000 m asl. The plain shows a gradual decrease in altitude towards the coast, with a regional tilt to the southeast.

Laguna de Santa Rosa is about 7 km long and up to 1 km wide (Figure 2). The mean altitude of the basin is 1520 m asl. At the time of drilling, the Laguna was dry. During the rainy season, parts of the Laguna are filled up to 1-2 m. In

August 1995, heavy rains associated with the Gabriela hurricane partly filled the Laguna. The slow infiltration and evaporation rates permitted to maintain the water levels through the winter season.

As part of the initial reconnaissance studies, a trench about 2.5 meters deep was excavated in the central-northern sector of Laguna de Santa Rosa. A dark gray clay deposit with abundant organic matter forms the shallow sequence with gasteropod remains. Geoelectrical studies were then carried out along a transect to determine the thickness of the lacustrine deposits and the basin shape (A. Musatov, written pers. comm., 1996). The apparent resistivity cross-sections were used to locate the fan coarse-grained and lacustrine fine-grained deposits, and select the location of the drilling site in the northern-central sector of the Laguna (Figure 2). We selected a site in the central sector away from the fan coarse-grained deposits (surface layers were investigated in the excavated trench). The drilling site is located at about 200 m away from the trench location.

LAGUNA DE SANTA ROSA SEQUENCE

The first 26 meters of the sedimentary sequence have been investigated by drilling with continuous core recovery (Figure 4). The drilling site was chosen in the northern-central sector of Laguna de Santa Rosa (coordinates: 24° 41.695' N, 99° 52.465' W), where the geoelectrical resistivity soundings indicated the occurrence of a thick lacustrine-clay sequence. This location was selected in order to core the fine grained sediments and avoid the input of coarse grained material and fan deposits which form a fluvial debris cone coming out from a small lateral valley.

The 26 m-sequence consists of a fairly homogeneous alternancy of clay units (Figure 4). Differences in the color, which ranges from black, green-gray, green-gray-brown to brown, permitted to distinguish ten clay units. Calcareous concretions of 1-2 cm size are present through the sequence, from about 4 m to 25 m. The first unit of a black to dark-gray color extends from surface to 3 m and contains a high degree

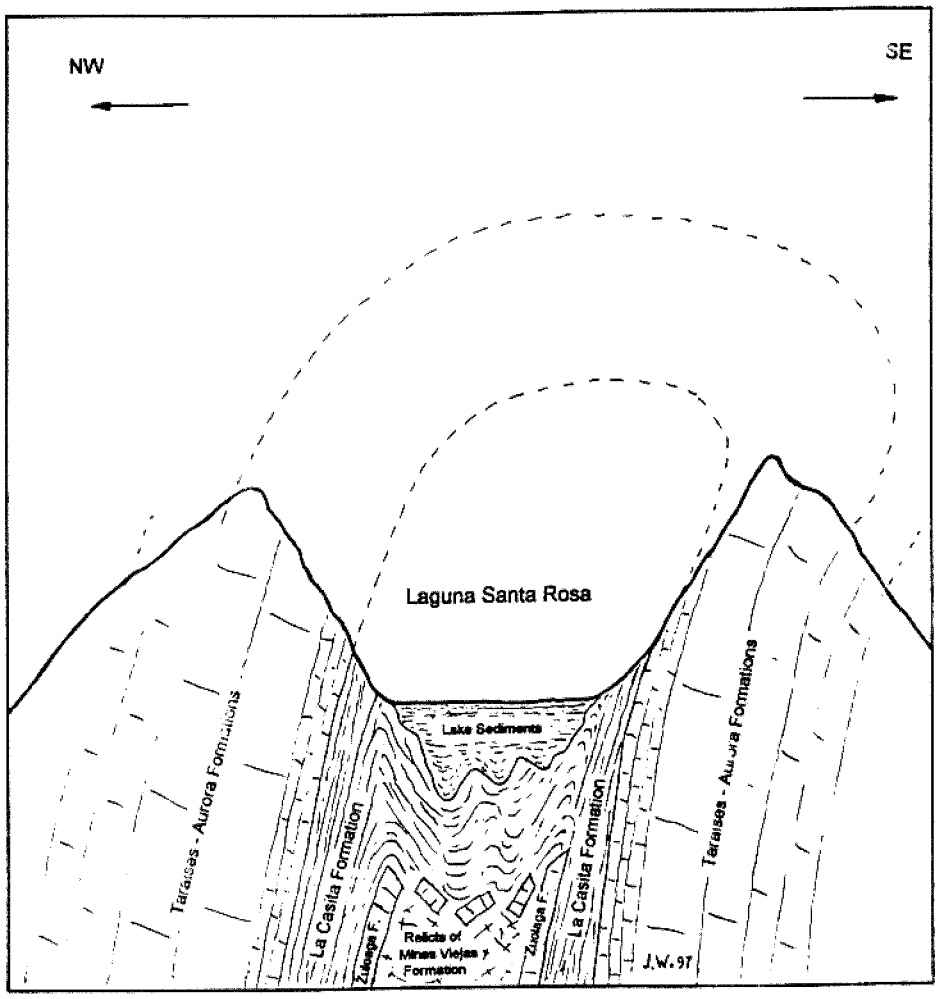

Fig. 3. Schematic cross-section through the Laguna de Santa Rosa basin showing the anticline structure and stratigraphy.

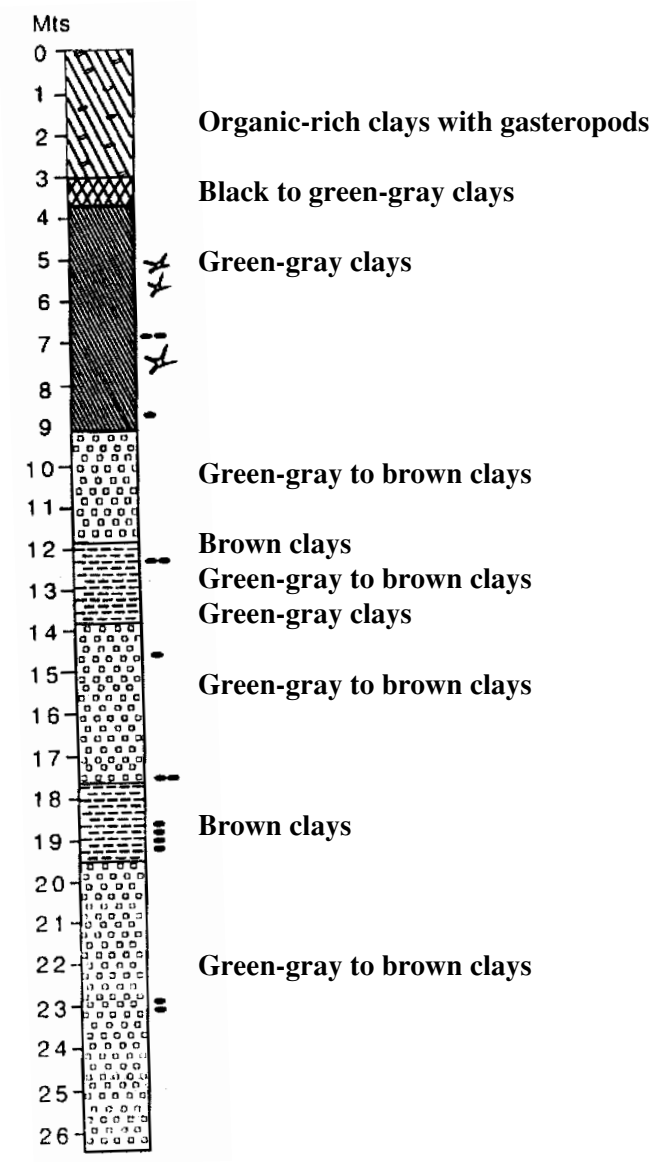

Fig. 4. Lithological column for the Laguna de Santa Rosa core with brief description of the clay sequence (see text for details).

of organic matter and gasteropod remains. Organic matter content decreases at depth through the whole sequence as indicated by a change in color. The second unit, some 0.6 m thick, grades from black to green-gray. The third unit of green-gray color is 5.5 m thick and shows irregular cavities filled with organic matter and calcareous concretions. The fourth unit is 2.7 m thick with green-gray-brown color. The fifth unit is a brown 1 m thick clay with calcareous concretions. The sixth unit is a green-gray-brown 0.8 m thick clay. The seventh unit is formed by thin 0.2-0.3 cm green-gray clays. The eight unit is a green-gray-brown 3.8 m thick clay with calcareous concretions. The ninth unit is a 1.8 m thick brown clay with calcareous concretions. The tenth unit extending from a depth of 19.5 m to the bottom of the core is a green-gray-brown clay.

MINERALOGY

Sample splits were processed for whole-rock and clay-mineral analyses at the Geochemical Laboratory of the University of Neuchâtel, Switzerland. Whole-rock and clay samples where analyzed with a Scintag XRD 2000, using analytical methods described in Kubler (1987). Whole-rock compositions were determined by XRD, based on methods by Ferrero (1966) and Kubler (1983). The method for semi-quantitative analysis of the bulk rock mineralogy (obtained by XRD patterns of random powder samples) used external standards.

Calcite, quartz, feldspars and phyllosilicates (Figure 5) mainly characterize whole-rock composition. Variations in these mineral contents and in the calcite/detritus ratio (calcite/quartz+phyllosilicates+feldspars) indicate that the Santa Rosa core can be mineralogically divided into three distinct major zones.

The upper zone (0-9 m) shows dominant quartz and phyllosilicates, with generally more than 20% calcite. Sporadic occurrences of plagioclase (albite) have also been recognized, but K-feldspars are nearly absent. The middle zone of the core (9-17.5 m) is enriched in quartz and phyllosilicates, whereas calcite is significantly decreased, thus indicating higher detrital input and/or reduced productivity (a cold and less humid interval, corresponding to a glacial interval ?). Among feldspars, only K-feldspar is present. The lower zone (17.5-26 m) is mineralogically similar to the first top 9 meters, and is again enriched in calcite and marked by the re-appearance of the plagioclase. These changes in mineralogical composition are therefore correlated with the low-field magnetic susceptibility data (see next section). The phyllosilicate fraction is mainly composed of mica, chlorite, smectite and kaolinite.

Shales and carbonates dominate the mineralogy of the catchment area. Whole-rock composition of the La Casita shales and Taraises limestones, which constitute the main detrital source for the Santa Rosa basin is relatively identical to the lake sediments composition (Adatte *et al*., 1996). Quartz, feldspars and phyllosilicates are more abundant in the shales of the La Casita Formation. The absence of kaolinite and smectite suggests that these Formations suffered deep burial diagenesis and tectonics. Kaolinite and smectite recognized in the lake sediments are therefore formed under coeval pedogenesis and can be used as paleoclimatic markers.

GEOCHEMISTRY, CARBON ISOTOPES AND RADIOCARBON DATING

Organic carbon and total carbonate contents were determined using a CS analyzer (Eltra, Metalyt-CS-1000-S).

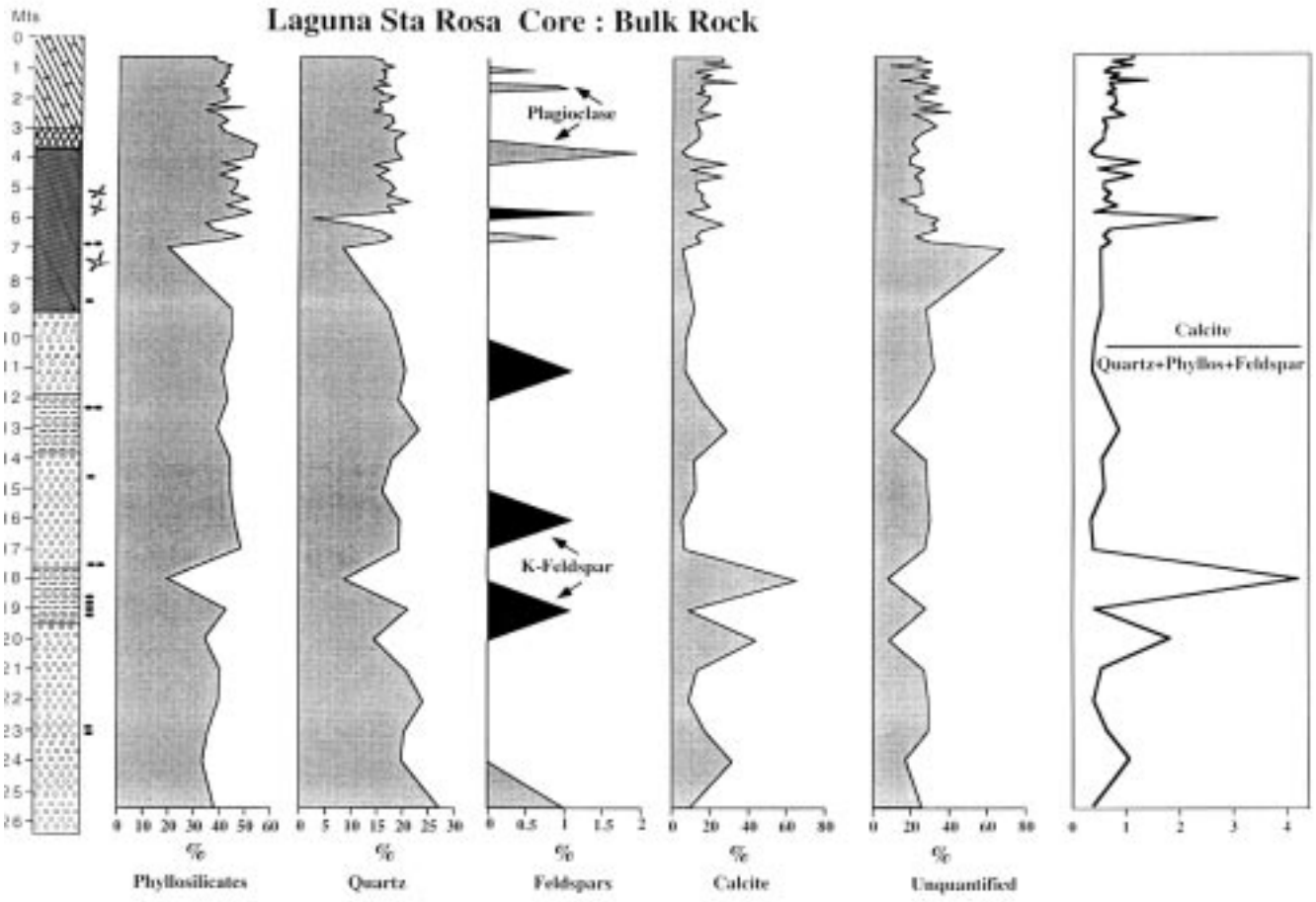

Fig. 5. Mineralogical data for the Santa Rosa core. (a) phyllosilicates, (b) quartz, (c) feldspars, (d) calcite, (e) unquantified, and (f) the calcite/detritus ratio (calcite/quartz+phyllosilicate+ feldspar).

In one step the total carbon content was determined, in a second step organic carbon was determined in a sample split in which carbonates were removed with hydrochloric acid (HCl). Standard deviation is less than 5% for samples with more than 1% and less than 10% for those with less than 1%C. The carbonate concretions present in several parts of the core (Figure 4) were not included for the calcium carbonate measurements.

Carbon isotope ratios of the organic carbon was determined using an elemental analyzer (Heraeus) coupled on-line to a Finnigan MAT Delta-S mass spectrometer. The isotope values are given as δ^{13} C values with respect to the V-PDB standard. Analytical precision is better than 0.1‰.

Results are summarized in Figure 6. With the exception of the upper three meters of the sequence, the organic carbon content is relatively low (less than 0.2 %). Due to this low content it was only possible to carry out AMS-C-14 dating in the uppermost samples. The carbonate content display significant differences in the lower, middle and upper part of the core. Lowest values (less than 1 %) occur in the upper zone 0-9 m, with highest values (above 2.5 %) being observed near the surface. The carbon isotopes δ^{13} vary from - 20.3 ‰ to -26.4 ‰ indicating changing conditions for organic carbon formation or alternatively, the input of different organic materials into the lake. Relatively uniform values that fluctuate slightly around –24 ‰ are observed below 11 m depth. In contrast, above this depth level, the isotopic values are more scattered and tend towards heavier values from 5 m towards the top of the core (Figure 6).

Samples were selected from various parts of the sequence for radiocarbon dating. Unfortunately, due to the low organic carbon contents in the clay units (Figure 6) only the samples from the first shallow unit were suitable for dating, even by using the accelerator mass spectrometry (AMS) method. Samples were analyzed in the Oxford Radiocarbon Accelerator Unit, University of Oxford by using the methods described in Hedges *et al*. (1989, 1992). The standard half-life of 5580 yr is used and dates are referred to AD 1950 (with 1-sigma errors) and corrected by natural

fractionation by reference to the δ^{13} C. AMS radiocarbon dates of (OxA-5628) 1525 +/- 75 yr B.P. and (OxA-6088) 5530 +/- 60 yr B.P. were obtained for samples at depths of 2 m and 3 m, respectively. The corresponding δ^{13} values for these samples are: -20.1 ‰ and -20.7 ‰, respectively (Hedges *et al.*, 1996). A preliminary apparent sedimentation rate that can be derived from these dates is about 25 mm/yr. If this sedimentation rate is representative for the deep units, then the 26 m core spans a considerable period (around 100 000 yr) of the Late Pleistocene and Holocene.

ROCK-MAGNETIC STUDY

Sediment samples were collected in the laboratory with standard non-magnetic 2.2x2.2x2.2 cm plastic cubes. Samples were spaced at different intervals ranging from 0.4 to 1 m. A total of 34 samples were used for the rock-magnetic study. Samples are weighted (to provide a normalization parameter for the magnetic measurements) and a rough estimate of bulk density could be derived from these measurements (Figure 7), which shows a rough correlation with the clay units (Figure 4). Density decreases at around 7 m, corresponding to a sample with irregular structures filled with organic matter. It is also low at about 18-20, 21-22 and 25 m.

The low-field magnetic susceptibility (k) was measured with the Bartington system equipped with the dual-frequency laboratory sensor. Measurements at low (470 Hz) and high (4700 Hz) frequencies permit investigation of the susceptibility spectrum. The low-field susceptibility shows low values of around 10 x 10^{-6} SI units at low (Figure 8a) and high (Figure 8b) frequencies. The susceptibility displays changes with depth that roughly correspond with the color changes of the clays. Low-field low-frequency susceptibility (k_{LF}) is slightly smaller in the first 8.5 m (around 10 x 10^{-6}

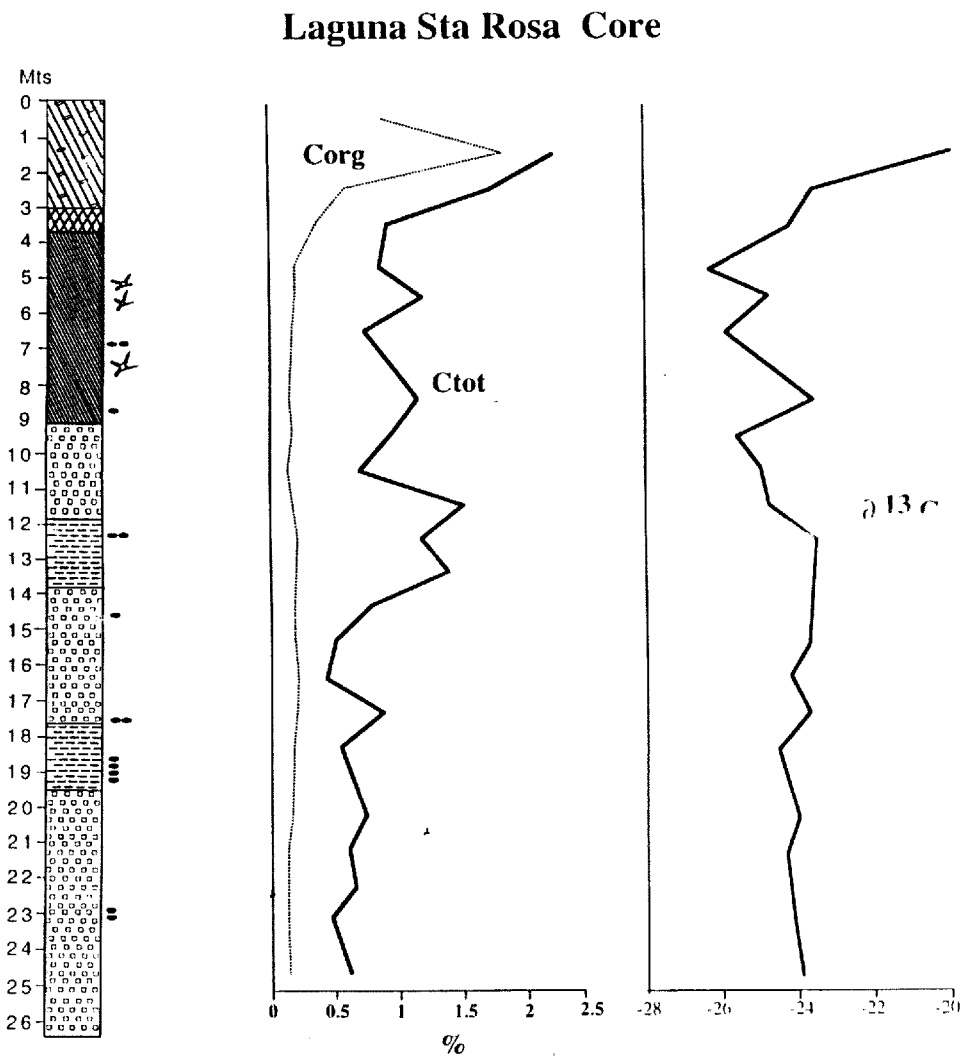

Fig. 6. (a) Organic carbon (Corg) and total carbon (Ctot) contents in the Laguna de Santa Rosa core. (b) Carbon isotopes (δ^{13} C) for the Laguna de Santa Rosa core.

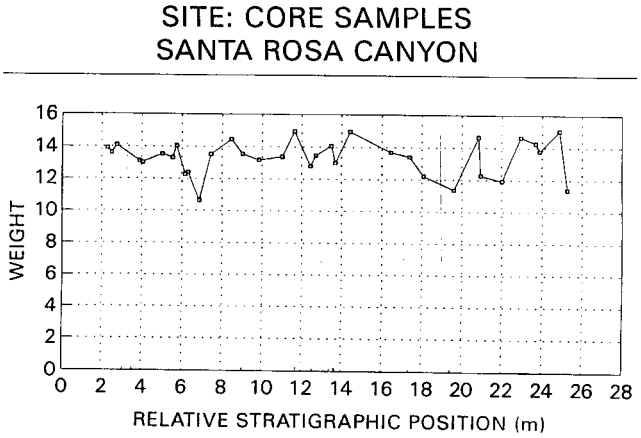

Fig. 7. Variation of density plotted as a function of depth NRM intensity plotted as a function of relative stratigraphic position.

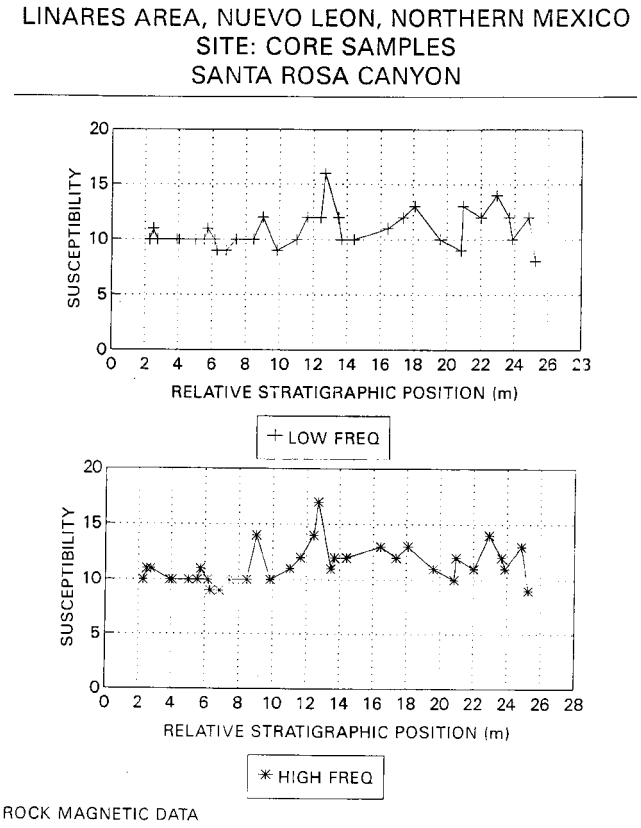

Fig. 8. Low-field magnetic susceptibility plotted as a function of relative stratigraphic position in the Santa Rosa core. (a) Low-frequency susceptibility and (b) High-frequency susceptibility.

SI) than in the deeper sections (around 12 x 10^{-6} SI). Low-field high-frequency susceptibility (k_{HF}) presents a similar pattern of variation with depth than the low-frequency measurements. There are no sharp peaks in the susceptibility records that could indicate any volcanic influence. Occurrence of tephra layers in the lacustrine sequences would greatly assist in reconstructing the stratigraphic relationships (this was one of the targets of the rock-magnetic study). The small susceptibility values suggest low contents of magnetic minerals (see also discussion below), which correlate with the magnetic properties of the lutites and carbonates of the Taraises and Aurora Formations, which form the topographic highs of the catchment area (Figure 3).

The intensity and direction of natural remanent magnetization (NRM) were measured with a Czech spinner JR-5 magnetometer. NRM intensity presents low values between 3.2 mA/m to 0.05 mA/m, with values fluctuating around 0.1 mA/m along the sequence (Figure 9). Two peaks are observed at about 2.8-3 m and 12.5-13 m. The peak at 12.5-13 m correlates with a peak observed in the susceptibility logs (Figure 8 a,b).

The susceptibility spectrum can be visualized in terms of the frequency dependent susceptibility variations, which can be expressed in percentage by the parameter of frequency dependence of susceptibility (k_{fd}):

$$k_{fd} = 100\ (k_{LF} - k_{HF})/k_{LF} \quad .$$

The susceptibility decreases with increasing measurement frequency, which reflects the interplay of the in-phase and out-of-phase (quadrature) components. The dependence on frequency can be used to investigate the magnetic mineralogy and grain size (and domain state) distribution (Bhathal and Stacey, 1969; Bloemendal *et al.*, 1985; Thompson and Oldfield, 1986; Maher, 1988; Hunt *et al.*, 1995). Measurements at two different frequencies are not sufficient to investigate the whole spectrum, and care is

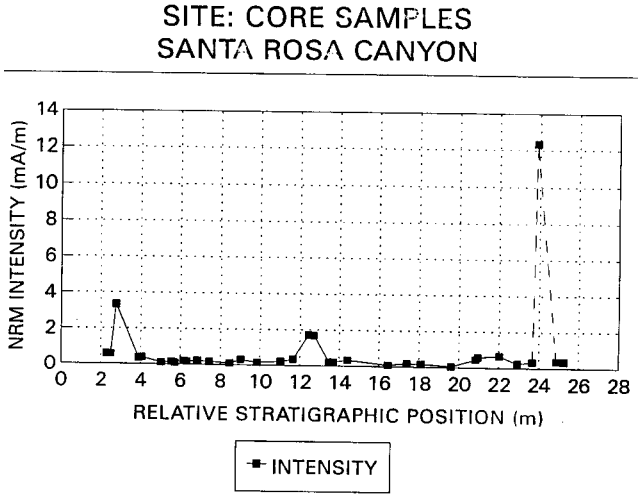

Fig. 9 Intensity of natural remanent magnetization (NRM) plotted as a function of relative stratigraphic position in the Santa Rosa core.

required to interpret results in terms of presence of superparamagnetic grains. In the Santa Rosa sequence, frequency dependence of susceptibility displays a larger degree of variability when plotted as a function of stratigraphic position (Figure 10), than the low- and high-frequency low-field susceptibility (Figure 8 a, b). The changes follow closely the different clay units previously identified mainly from changes in the color along the core (Figure 4). Other properties like the density and low-field susceptibility show a rough correspondence with the color changes of the clays, in detail there are however some discrepancies, with density and susceptibility changes that do not correspond to color changes (Figures 7 and 8). The relatively low values of magnetic susceptibility and NRM intensity observed in the different clay units along the core points to a small amount of magnetic minerals. The close correlation between the frequency dependence of susceptibility and the clay units suggests that the susceptibility also reflects grain size variations (which influences the ability of magnetic grains to respond to variable-frequency applied fields).

Further investigation of the magnetic mineralogy and domain state was accomplished by giving the samples an isothermal remanent magnetization (IRM). IRM was given in steps by application of direct fields up to a maximum field of 500 mT with a pulse magnetizer. The saturation or the maximum IRM was subsequently demagnetized by application of alternating fields (AF) with a Schonstedt demagnetization instrument. AF demagnetization was carried out in steps with the stationary three orthogonal axes method up to maximum fields of 100 mT. Some samples show IRM acquisition curves that reach saturation in low fields, whereas other samples do not attain saturation up to 500 mT. The response to direct fields is dominated by the presence of low coercivity titanomagnetites. Normalized intensity AF demagnetization curves also indicate the predominance of low coercivity minerals plus the occurrence of a variable amount of higher coercivity minerals. The high coercivity fraction is represented by the percentage of the magnetization still remaining after demagnetization to 100 mT (estimated with respect to the initial NRM intensity). This varies from less than 5 % up to 25-40 %. The high coercivity fraction may correspond to goethite. The brownish coloration in some of the clay units (e.g., below 9.2 m) suggests the occurrence of goethite and lepidocrocite. Selected samples were further analyzed by using a MicroMag instrument for measuring the magnetic hysteresis (Figure 11) and direct and demagnetization reverse field IRM (Figure 12). Hysteresis curves show saturation in low applied fields (Figure 11). A plot (Figure 13) of the ratios of remanent magnetization/ saturation magnetization (Mr/Ms) as a function of the coercivity ratios of coercivity/coercivity of remanence (Hc/ Hcr) indicates that the magnetic carriers mainly fall within the pseudo-single domain field (Day *et al*., 1977). Additional

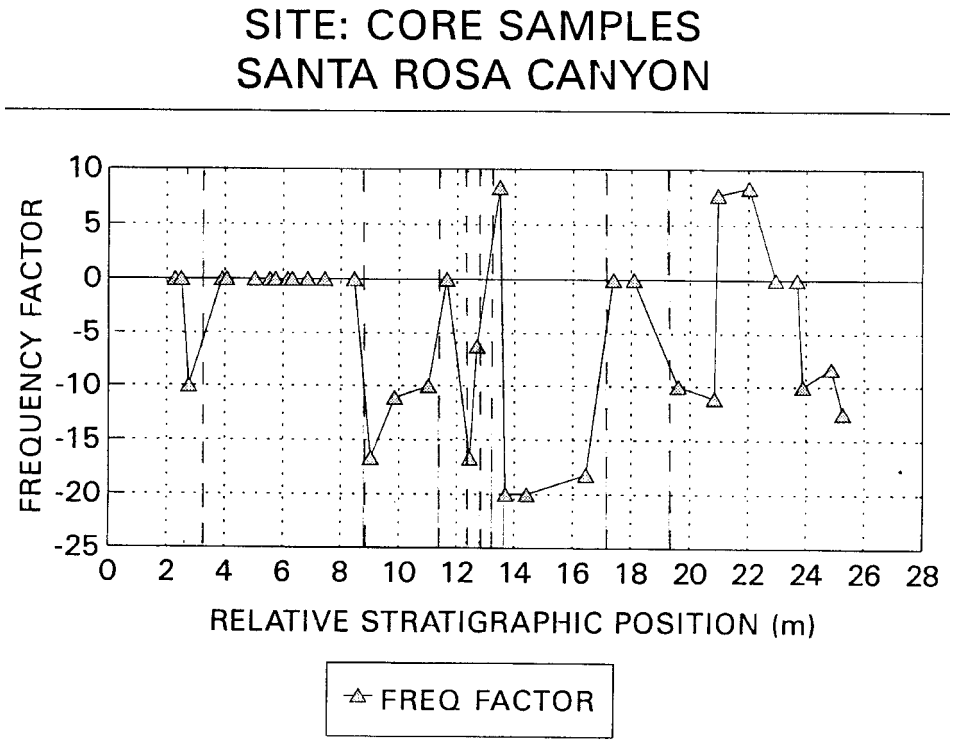

Fig. 10. Frequency dependence of magnetic susceptibility plotted as a function of relative stratigraphic position for the Santa Rosa core.

rock-magnetic property studies are required to investigate the magnetic mineralogy of the sequence.

DISCUSSION

In the past few years, investigation of magnetic minerals and properties of lacustrine sediments has been increasingly applied to paleoenvironmental and paleoclimatic studies (Thompson and Oldfield, 1986). Lacustrine basins are to a large degree material-bounded with close lake-watershed ecosystems, thus providing spatially finite and convenient subjects of study. The lacustrine sedimentary record often preserves information concerning the characteristics and processes of the catchment basin (e.g., topography, slope processes, lithologies, material flux, vegetation cover, tectonics and erosional processes), and climatic changes (e.g., from seasonal to long-term changes). Magnetic minerals in lake sediments are usually classified in terms of their origin into: authigenic, diagenetic and allogenic. Authigenic minerals form in situ by chemical or biogenic processes. Diagenetic minerals are those resulting from transformation of existing minerals. Allogenic minerals originate outside the lake, and can come from nearby or distant sources. Magnetic minerals generally constitute a small percentage of the bulk lake sediment, and study of the magnetic properties of sediments allows investigation of the magnetic mineralogy, grain size, sediment source, erosion and transport, and diagenetic processes (e.g., Thompson *et al*., 1975; Dearing *et al*., 1981; Thompson and Oldfield, 1986; Snowball and Thompson, 1990; Peck *et al*., 1994; Ortega-Guerrero *et al*., 2000).

The lacustrine sequence of Laguna de Santa Rosa is formed by a fairly homogenous alternancy of clay units. The sequence was formed as a mixture of clastic clay suspension and chemically precipitated calcium carbonate, in a shallow ephemeral lake. There are no coarse-grained sediments and the only observable macroscopic changes are in the color of the clays (Figure 4). The characteristics of the clays without any observable fine stratification suggest relatively tranquil

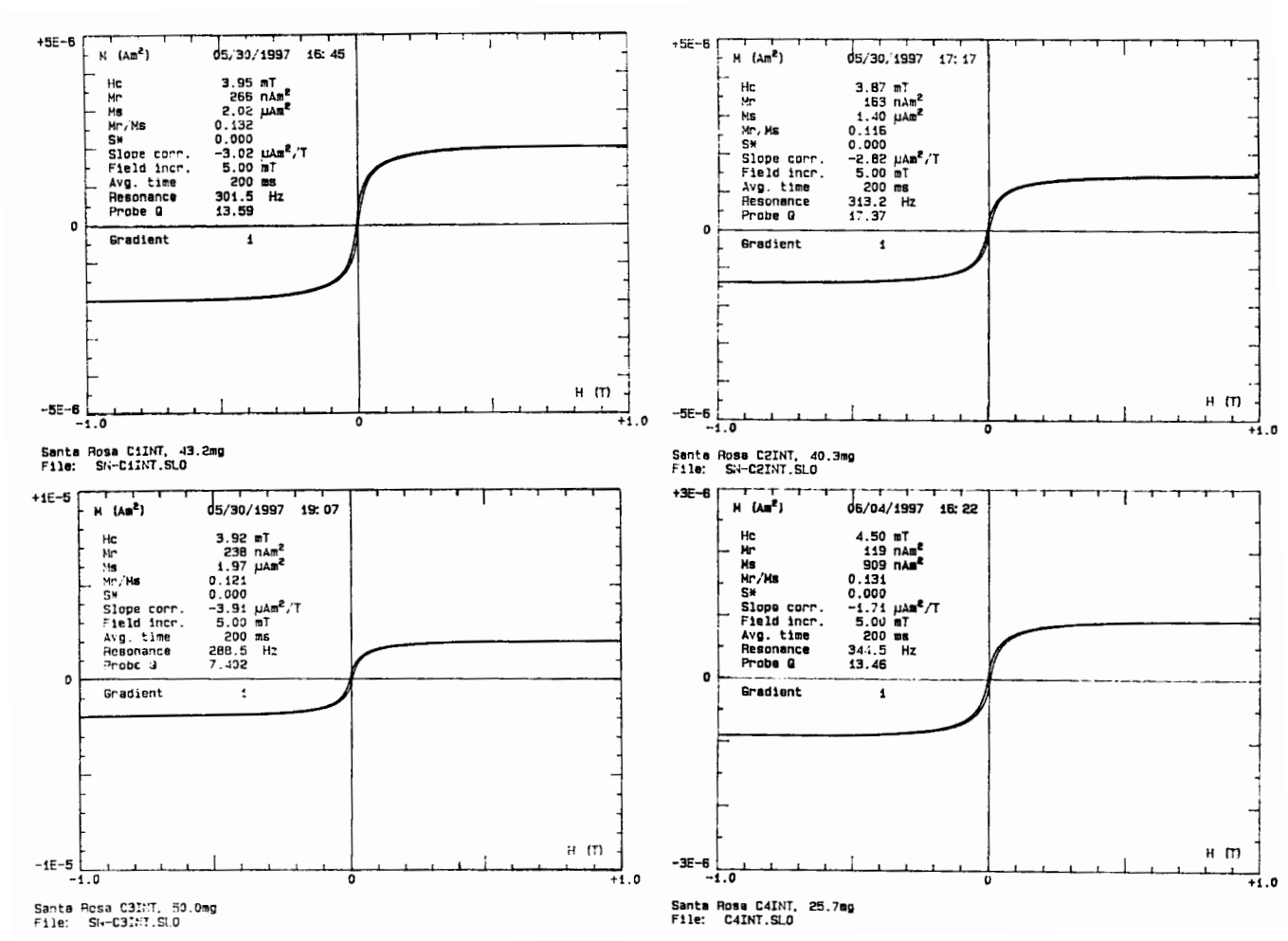

Fig. 11. Examples of magnetic hysteresis loops for four samples of the Laguna de Santa Rosa sequence. The magnetic hysteresis parameters are summarized in the table annexed to the graphs. Magnetic field increment used is 5 mT. Measurements performed in a MicroMag instrument.

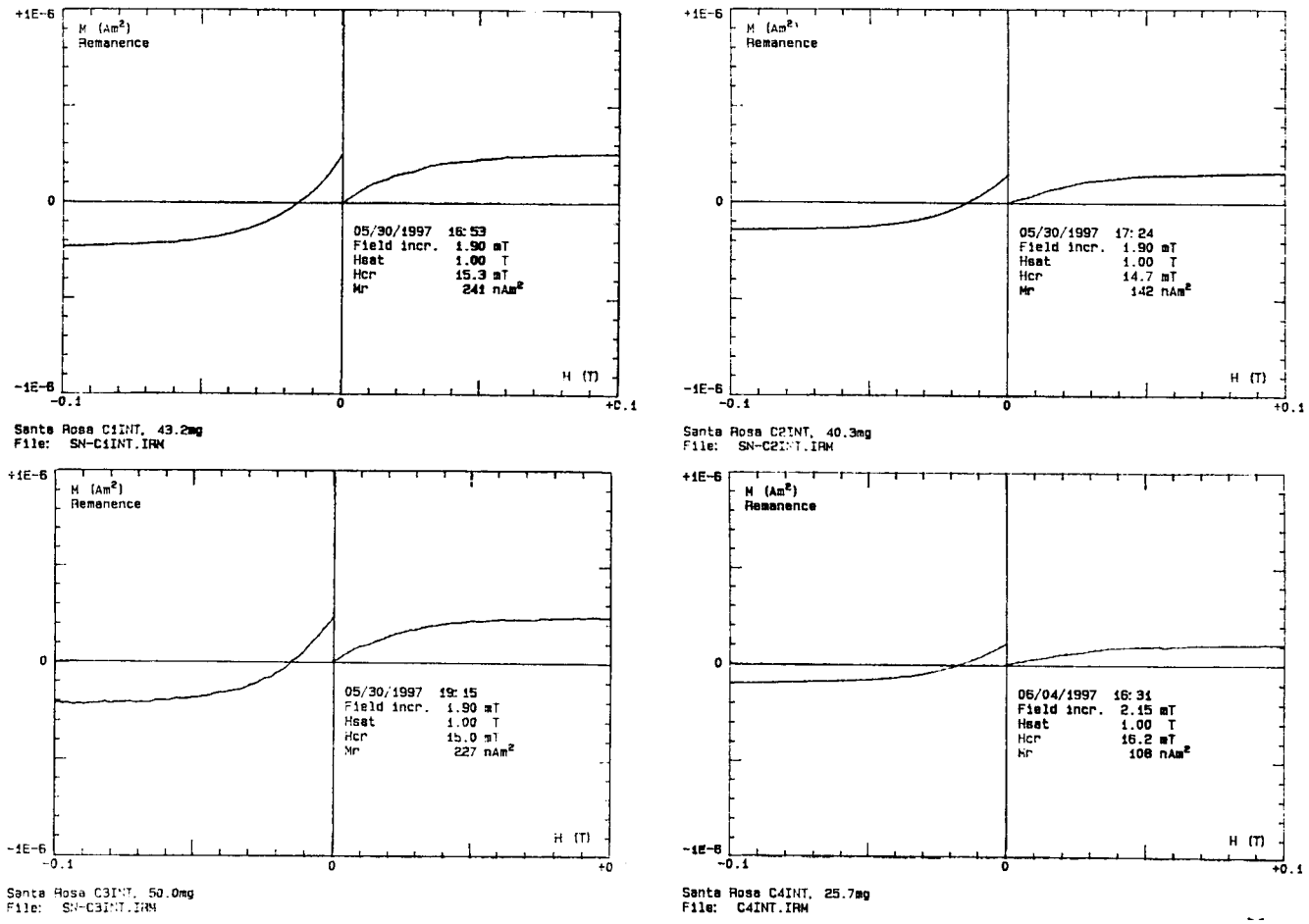

Fig. 12. Examples of isothermal remanent magnetization (IRM) acquisition curves and reverse field demagnetization curves for four samples of the Laguna de Santa Rosa core.

and stable conditions in the catchment basin, with no indications of major erosional and depositional perturbations like those associated with extreme events. The susceptibility (Figure 8 a, b) and NRM intensity (Figure 9) present low values in the different units, which suggests a relatively low content of magnetic minerals. Previous studies of lacustrine sequences in European regions have shown that magnetic minerals are dominantly allogenic (e.g., Dearing *et al.*, 1981; Dearing and Flower, 1982; Thompson and Oldfield, 1986; Snowball, 1993; Peck *et al.*, 1994). This may also be the case in the Laguna de Santa Rosa, and magnetic minerals came from the surrounding lutites and carbonate rocks and transported into the lake. This is supported by the low values of magnetic susceptibility and NRM intensity in the clay units and the similarities in magnetic properties (coercivity spectra) observed in the carbonates of the Taraises and Aurora Formations, which form the catchment area (J. Urrutia-Fucugauchi, D.H. Tarling and A.M. Soler, unpublished paleomagnetic data 1996). There are however indications that authigenic minerals can be important in some lacustrine sediments. For instance, iron sulfide phases like gregite (Fe_3S_4) have been documented in recent sediments deposited under sulfate-reducing conditions (e.g., Snowball and Thompson, 1990). There is no indication in the rock magnetic record of volcanic derived material interbedded in the clay units.

The variation of the frequency dependence of susceptibility with stratigraphic position closely follows the changes in color of the clays (Figure 10). This correlation suggests that the color is related to the magnetic and iron-rich minerals in the clays. This relationship may not necessarily be a direct one; that is, that the color is the result of the same magnetic mineral responsible for a given value of the frequency dependence of susceptibility. In fact, there are indications that the relation is indirect. For instance, the black color of the shallow unit down to 3 m depth is associated with a high content of organic matter (Figure 6). The organic matter content in the rest of the sequence is low and fairly uniform. This shallow unit shows no susceptibility variation

with frequency (k_{fd} = 0 %). This 0 % value of k_{fd} is also the case with the third 5.5 m thick unit and three other thin units at deeper levels (Figure 10). The other units are characterized by a variation in the frequency dependence of susceptibility; two thin units show positive values of about 8 % and the rest show negative values around 10 % and up to -20 %. The brown colors observed in the clays at 11.8-12.8 m and 17.7-19.5 m may be associated with iron-hydroxides. Iron-hydroxides such as goethite and perhaps lepidocrocite may also be present in the clay units below 9.2 m as suggested by the brownish coloration (Figure 4).

The magnetic susceptibility measured at low fields gives an estimate of how a material responds to the applied magnetic field. In general, it is taken as a simple measure on the amount of magnetic minerals (particularly for ferrimagnetic iron-titanium oxides) present in a sample. However, this relationship is not always a simple one, and additional factors may need to be considered (e.g., in mixtures of various magnetic minerals with wide ranges of grain sizes). In ferrimagnetic (e.g., magnetite) and canted antiferromagnetic (e.g., hematite) minerals, the susceptibility depends on grain size and shape; e.g., for crushed magnetite grains, susceptibility doubles between 1 μm and 100 μm, and for grown magnetite grains, susceptibility increases one-third between 0.03 μm and 10 μm (Hunt *et al*., 1995). For ultrafine-grained minerals the variations may be large, particularly around the transition region between superparamagnetic and single-domain grains. For instance, the susceptibility of grown magnetite grains smaller than 20 nm is twice that of grains larger than 30 nm (Hunt *et al*., 1995). When sediments present a narrow range of grain sizes, the susceptibility depends

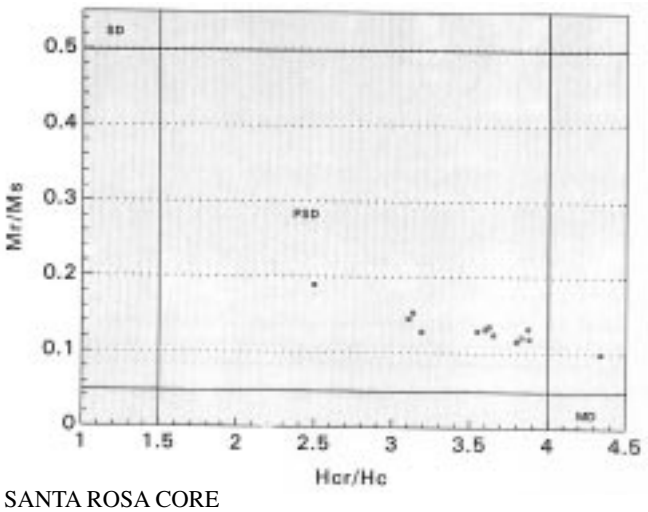

SANTA ROSA CORE

Fig. 13. Magnetic hysteresis diagram showing the remanent magnetization/saturation magnetization ratio (Mr/Ms) plotted as a function of the coercivity/coercivity of remanence ratio (Hc/Hcr). Note that the samples fall dominantly within the pseudo-single domain (PSD) field. The two other fields are for single domain (SD) and multidomain (MD) states.

mainly on the amount of magnetic minerals; however, if there is a wide range of grain sizes this dependence on amount of magnetic minerals is not direct. The frequency dependence of susceptibility has been used to distinguish ultrafine-grained magnetite and maghemite (Thompson and Oldfield, 1986). Superparamagnetic grains can be detected from the correlation between Rayleigh loops and the frequency dependence of susceptibility (Bloemendal *et al*., 1985). Magnetite grains near 20 nm contribute to susceptibility at low-frequencies but not at high-frequencies (Maher, 1988; Hunt *et al*., 1995).

Because of the low organic matter contents in the clay sequence (Figure 6), only three radiocarbon dates were obtained from the upper part of the sequence (two in the core and one in a nearby trench). The dates of 1525 and 5530 yr B.P. are obtained from the (core) depths of 2 m and 3 m, respectively, suggest slow sedimentation rates. Although, it is not possible to reliably estimate the time represented by the 26 m thick sequence and corresponding sedimentation rates, extrapolation of the radiocarbon data suggests that the 26 m sequence could cover a considerable period into the Late Pleistocene.

In the region of the Sierra Madre Oriental, only those areas with high elevations were likely affected by glaciation in the Late Pleistocene. Field studies conducted by J. Werner have located an outcrop of glacial morraine deposits in a zone 40 km northeast of the Laguna de Santa Rosa in the Cerro Potosi, at an altitude of about 3500 m asl (Oropeza, 1990; J. Werner *et al*., unpublished data).

Pollen and diatom studies have been completed as part of the interdisciplinary project on samples from the Santa Rosa core. Analyses of diatoms through the clay sequence indicate that these silica microfossils have not been preserved or were not present during the evolution of the lake (M. Caballero-Miranda, written pers. comm., 1996). Pollen analysis also indicates a poor degree of preservation, which is a major limitation in studying the paleoenvironmental and paleoclimatic evolution of the basin (J. Jones, written pers. comm., 1996).

The stratigraphic variations of rock-magnetic properties (Figures 8 to 10), carbonate content and isotopic carbon (Figure 6) and mineralogy (Figure 5) roughly define three major zones. These zones are separated by peaks of the calcite to quartz + phyllosilicate + feldspar ratio (the calcite/detritus ratio). The phyllosilicate fraction is mainly composed of mica, chlorite, smectite and kaolinite. The upper zone extends to a depth of about 7-9 m formed by three clay units: the organic clay with abundant gasteropods and two black to green gray clays. This zone is characterized by magnetic susceptibilty values around 10^{-6} SI, frequency dependent factors of about 0 %, δ^{13} C values ranging from -20.3 ‰ at the surface to

-26.4 ‰, presence of quartz and phyllosilicates with generally more than 20 % calcite, sporadic occurrence of plagioclase (albite) and K-feldspars nearly absent. The middle zone that extends from 9 m to 17.5 m, formed by five clay units with colors ranging from green gray to brown. This zone is characterized by higher variable susceptibility values up to 17 10^{-6} SI, negative frequency dependent factors, and low (around 1 %) total carbon contents. This zone is enriched in quartz and phyllosilicates, with less calcite, indicating a higher detrital input and/or reduced productivity (corresponding to a cold and less humid interval). The lower zone extending from 17 m to 26 m and formed by two brown to green gray clay units. This zone is characterized by high variable magnetic susceptibility, variable frequency dependent factors, total carbon contents with two peaks > 4 % at about 18 and 20.5 m and δ^{13} values around -24 ‰. Its mineralogy is similar to the shallow zone, again enriched in calcite and with occurrence of plagioclase.

There is relatively little information concerning the paleoclimatic evolution of northeastern Mexico during the Late Pleistocene and Holocene (e.g., Ortega-Ramírez *et al*., 1998; Urrutia-Fucugauchi *et al*., 1997a, b). Forman *et al*. (1995) have proposed a paleosynoptic scenario for the mid-continental and eastern United States with aridity episodes during the full glacial and mid-Holocene 6000 yr B.P. and intervals of landscape stability with precipitation levels similar to present at the time of last deglaciation and at about 3000 yr B.P. The paleoclimatic evolution is related to the disappearance of the Laurentide ice sheet, the splitting and shifts of the Jet Stream and relative positions of major pressure highs and lows, particularly the shifts of the Bermuda High (Figure 14). During the Hypisithermal (6000 yr B.P.) location of Jet Stream shifted to the north while the Bermuda High moved to the northeast; which resulted in changes in precipitation patterns in northeastern Mexico and the High Plains of central and southeastern United States. The lack of a detailed chronology for the Santa Rosa core does not permit to analyze the data in terms of a regional paleoclimatic model. One may speculate that the upper zone corresponds to the Holocene and spans the paleoclimatic changes with the mid-Holocene 6000 yr B.P. drought and the 3000 yr B.P. humid conditions. Extrapolation of the radiocarbon dates for a depth of about 9 m, gives a temporal estimate consistent with the Holocene-Pleistocene transition. In the Laguna de Santa Rosa core, the middle zone (9-17.5 m) characterized by high detrital input and/or reduced productivity may then span the Late Pleistocene glaciation with cold and less humid conditions, with the splitting and southerly drift of the Jet Stream.

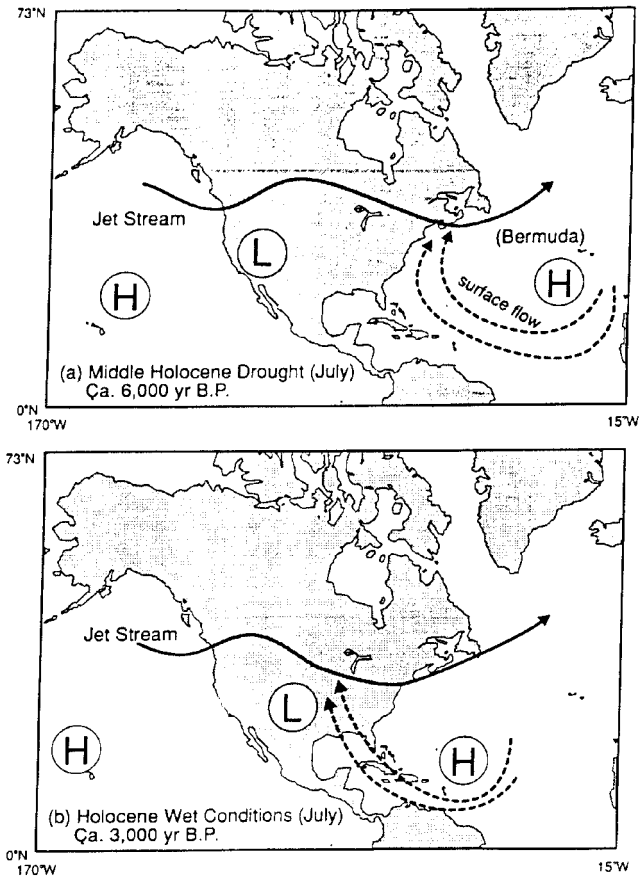

Fig. 14. Simplified inferred mean July upper-level (300 to 700 mb) atmospheric circulation patterns with location of the Jet Stream and Bermuda High at (a) 6000 yr B.P., middle Holocene drought conditions, and (b) 3000 yr B.P., late Holocene wet conditions. Eastward displacement of the Bermuda and Western US Highs blocks entrance of moisture-laden flow resulting in regional drought in middle Holocene times. In the late Holocene the Bermuda High is displaced westwards into southern US and Gulf of Mexico and the ridge aloft over western US weakens, permitting entrance of moisture-laden flow in the Gulf area (adapted from Foreman *et al*., 1995).

ACKNOWLEDGMENTS

This study forms part of the Linares research project on the paleoclimatic evolution of northeastern Mexico. We gratefully acknowledge the assistance and many useful discussions of the project participants. V. Baker, A. Musatov, J. Jones, W. Stinnisbeck, A.M. Soler and M. Caballero participate in the project and provided unpublished data, which has been useful in preparing this paper. Technical support by J. Richard and A.M. Soler in the mineralogical and magnetic analyses is gratefully acknowledged. Comments by two anonymous referees and P. Vlag have been useful in preparing this paper. Partial economic support is provided by grants from Institute of Geophysics, UNAM, National Council of Science and Technology (CONACYT-3207-T), University of Nuevo Leon, International Agency of Atomic Energy (8812/RB), Alfred-Wegner Institute, the BMBF, Germany and European Community (project CI1-CT94-0114).

BIBLIOGRAPHY

ADATTE, T., W. STINNISBECK, J. REMANE and W. H. HUBBERTEN, 1996. Paleoceanographic changes at the Jurassic-Cretaceous boundary in the Western Tethys, northeastern Mexico. *Cretaceous Res., 17,* 671-689.

BHATHAL, R. S. and F. D. STACEY, 1969. Frequency independence of low field susceptibility of rocks. *J. Geophys. Res., 74,* 2025-2027.

BLOEMENDAL, J., C. BARTON and C. RADHA-KRISHNAMURTY, 1985. Correlation between Rayleigh loops and frequency-dependent and quadrature susceptibility: Application to magnetic granulometry of rocks. *J. Geophys. Res., 90,* 8789-8792.

BRADBURY, J. P., 1997. Sources of full and late glacial moisture in Mesoamerica. *In:* Urrutia-Fucugauchi, J., Metcalfe, S. and Caballero-Miranda, M. (Eds). Climatic Change in Mexico, Quat. Intern., 43/44, 97-110.

CARLSEN, T. W., 1987. Stratigraphy and structural traverse of Santa Rosa canyon, Nuevo Leon, Mexico. Actas Fac. Ciencias de la Tierra, Univ. Nuevo León, 2, 205-212.

DAY, R., M. D. FULLER and V. A. SCHMIDT, 1977. Hysteresis properties of titanomagnetites: grain size and composition dependence. *Phys. Earth Planet. Inter., 13,* 260.

DEARING, J. A. and R. J. FLOWER, 1982. The magnetic susceptibility of sedimenting material trapped in Lough Neagh, northern Ireland, and its erosional significance. *Limnol. Oceanogr., 27,* 969-975.

DEARING, J. A., J. K. ELNER and C. M. HAPPEY-WOOD, 1981. Recent sediment influx and erosional processes in a Welsh upland lake-catchment based on magnetic susceptibility measurements. *Quat. Res., 16,* 356-372.

DEKKERS, M. J., 1988. Some rockmagnetic parameters for natural goethite, pyrrhotite and fine-grained hematite. Geol. Ultraiectina, 51, 231 pp.

DUNLOP, D. J., 1986. Hysteresis properties of magnetite and their dependence on particle size. *J. Geophys. Res., 91,* 9569-9584.

FERRERO, J., 1966. Nouvelle méthode empirique pour le dosage des minéraux par diffraction R.X. Bordeaux; France. Rapport Compagnie Française des Pétroles, Unpublished Report. 32pp.

FORMAN, S. L., R. OGLESBY, V. MARKGRAF and T. STAFFORD, 1995. Paleoclimatic significance of Late Quaternary eolian deposition on the Piedmont and High Plains, Central United States. *Global Planet. Change, 11,* 35-55.

HEDGES, R. E. M., I. A. LAW, C. R. BRONK and R. A. HOUSLEY, 1989. The Oxford accelerator mass spectrometry facility: technical developments in routine dating. *Archaeometry, 31,* 99-114.

HEDGES, R. E. M., M. J. HUMM, J. FOREMAN, G. J. VAN KLINKEN and C. R. BRONK, 1992. Developments in sample combustion to carbon dioxide in the Oxford AMS carbon dioxide ion source system. *Radiocarbon, 34,* 306-311.

HEDGES, R. E. M., P. B. PETTITT, C. B. RAMSEY and G. J. VAN KLINKEN, 1996. Radiocarbon dates from the Oxford AMS system: Archaeometry datelist 22. *Archaeometry, 38,* 391-415.

HILTON, J. and J. P. LISHMAN, 1985. The effect of redox change on the magnetic susceptibility of sediments from a seasonally anoxic lake. *Limnol. Oceanogr., 30,* 907-909.

HUNT, C. P., M. J. SINGER, G. KLETETSCHKA, J. TENPAS and K. L. VEROSUB, 1995. Effect of citrate-bicarbonate-dithonite treatment on fine-grained magnetite and maghemite. *Earth Planet. Sci. Lett., 130,* 87-94.

KUEBLER, B., 1983 Dosage quantitatif des minéraux majeurs des roches sédimentaires par diffraction X. Cahiers de l´Institut de Géologie de Neuchâtel, Série AX, 1.1., 12pp.

KUEBLER, B., 1987 Cristallinitité de l´illite, méthodes normalisées de préparations, méthodes normalisées de mesures. Cahiers de l´Institut de Géologie de Neuchâtel, Série ADX, 1.1., 13 pp.

MAHER, B. A., 1988. Magnetic properties of some synthetic submicron magnetites. *Geophys. J., 94,* 83-96.

OROPEZA, O. O., 1990. Depósitos periglaciales y erosión de suelos en el Cerro El Potosí, Mpio. de Galeana, N.L., México. Mem. Primer Simp. Nac. Degradación del Suelo, Instituto de Geología, UNAM, México, 21-22.

ORTEGA-GUERRERO, B., R. THOMPSON and J. URRUTIA-FUCUGAUCHI, 2000. Magnetic properties

of lake sediments from Chalco Lake, central Mexico, and their palaeoenvironmental implications. *J. Quat. Sci., 15,* 127-140.

ORTEGA-RAMÍREZ, J., A. VALIENTE-BANUET, J. URRUTIA-FUCUGAUCHI, C. MORTERA and G. ALVARADO-VALDEZ, 1998. Paleoclimatic changes during the Late Pleistocene-Holocene in Laguna Babicora, near the Chihuahuan Desert, Mexico. *Can. J. Earth Sci., 35,* 1108-1179.

PADILLA Y SÁNCHEZ, R., 1978. Bosquejo geológico estructural de la Sierra Madre Oriental en el area Linares-Galeana-San Roberto, Estado de Nuevo León. *Rev. Inst. Geol., UNAM, 2,* 45-54.

PECK, J. A., J. W. KING, S. M. COLMAN and V. A. KRAVCHINSKY, 1994. A rock magnetic record from Lake Baikal, Siberia: Evidence for a Late Quaternary climatic change. *Earth Planet. Sci. Lett., 122,* 221-238.

RUIZ-MARTÍNEZ, M. A. and J. WERNER, 1997. Quaternary sediments and climatic changes in northeastern Mexico. *In:* Urrutia-Fucugauchi, J., Metcalfe, S., and Caballero-Miranda, M., (Eds), Climatic Change in Mexico, Quat. Intern., 43/44, 145-151.

SÁNCHEZ-ÁLVAREZ, R. and J. URRUTIA-FUCUGAUCHI, 1992. Shallow crustal structure and palaeotectonics of northern Mexico. Volumen, Congreso Latinoamericano de Geología, Salamanca, España.

SNOWBALL, I., 1993. Mineral magnetic properties of Holocene lake sediments and soils from the Kara Valley, Lappland, Sweden, and their relevance to paleoenvironmental reconstructions. *Terra Nova, 5,* 258-270.

SNOWBALL, I. and R. THOMPSON, 1990. A stable chemical remanence in Holocene sediments. *J. Geophys. Res., 95,* 4471-4479.

THOMPSON, R. and F. OLDFIELD, 1986. Environmental Magnetism. Allen and Unwin, London, UK, 227 pp.

THOMPSON, R., R. W. BATTARBEE, P. E. O'SULLIVAN and F. OLDFIELD, 1975. Magnetic susceptibility of lake sediments. *Limnol. Oceanogr., 20,* 687-698.

URRUTIA-FUCUGAUCHI, J., J. ORTEGA-RAMÍREZ and R. CRUZ-GATICA, 1997a. Rock-magnetic study of Late Pleistocene-Holocene sediments from the Babicora lacustrine basin, Chihuahua, northern Mexico. *Geofís. Int., 36,* 77-86.

URRUTIA-FUCUGAUCHI, J., S. METCALFE and M. CABALLERO, (Eds), 1997b. Climatic Change in Mexico. *Quat. Intern., 43/44,* 1-190.

J. Urrutia-Fucugauchi[1], M.A. Ruiz-Martínez[2], J. Werner[3], H.-W. Hubberten[4], T. Adatte[5], E. Escobar-Hernández[1], A. Arciniega-Ceballos[1], M. Hernández[2] and A. De León[3]

[1] Laboratorio de Paleomagnetismo y Geofísica Nuclear, Instituto de Geofísica, Universidad Nacional Autónoma de México, Del. Coyoacán 04510 D.F., MÉXICO

[2] Facultad de Ciencias Forestales, Universidad Autónoma de Nuevo León, Linares 67700, Nuevo León, MÉXICO

[3] Facultad de Ciencias de la Tierra, Universidad Autónoma de Nuevo León, Linares 67700, Nuevo León, MÉXICO

[4] Alfred-Wegner Institut für Polar-und Meeresforschung, Forschungsstelle Potsdam, Telegrafenberg A43, D-14473 Potsdam, GERMANY

[5] Institut de Géologie, Université de Neuchâtel, 11 rue Emile Argand, 2007 Neuchâtel, SWITZERLAND